Table 1.
Synthesis of oligo (lactic acid) macromonomers

Code	Chemical composition in feed (mmol)		[Lactide]/ [HEMA]	Chirality	Atmosphere	Pressure (atm)	Reprecipitation solvent	Polymerization degree (n)	Yield (%)
	HEMA	Lactide							
OLLA12	12	69	6.75	L	Argon	1.0	2-Propanol/ Hexane = 1:1	14	46
OLLA20	6.9	69	10	L	–	0.0013	Ethanol/ Hexane = 1:1	21	67
OLLA30	4.6	69	15	L	–	0.0013	Methanol	34	71
ODLA12	12	69	6.75	D	Argon	1.0	2-Propanol/ Hexane = 1:1	13	40
ODLA20	6.9	69	10	D	–	0.0013	Ethanol/ Hexane = 1:1	19	76
ODLA30	4.6	69	15	D	–	0.0013	Methanol	33	80

Polymerization degree was determined by ^{1}H-NMR.

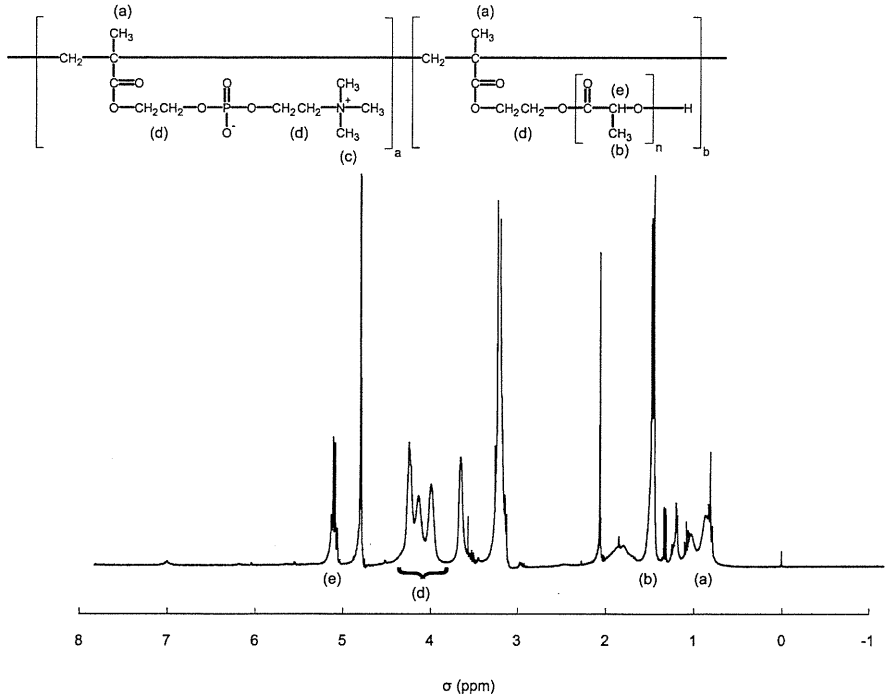

Figure 1. ^{1}H-NMR spectrum of a representative PMLA (X-PMDLA20-5).

PBS at a specific release time)/(theoretical maximum fluorescence intensity calculated from the amount of FITC-labeled BSA)× 100; this ratio was then plotted against time.

3. Results and Discussion

3.1. Synthesis of MPC Polymers with OLA as a Side-Chain

The MPC polymers (PMLA) were prepared to develop a water-soluble graft polymer with an oligo(lactic acid) side-chain. These polymers cause spontaneous gelation in aqueous solutions, which can be attributed to the formation of a stereocomplex between OLLA and ODLA. Biologically active substances can be incorporated in the polymer hydrogel during gelation, and the gel generally degrades under physiological conditions due to the non-enzymatic hydration of oligo(lactic acid) chains. During the degradation process, the biologically active substances incorporated in the hydrogel may be released. De Jong *et al.* reported self-assembled hydrogel using that system [4–6]. They grafted OLLA (dex-(L)lactate) and ODLA (dex-(D)lactate) to dextran and it is observed that the mixture of dex-(L)lactate aqueous solution and dex-(D)lactate aqueous solution formed a hydrogel. However, the various functions are required to the biomaterial and those are achieved by the controlled polymerization of the various monomers. From this point of view, polymethacrylate is

more suitable than polysaccharide because there are many methacrylate monomers and we can co-polymerize them. Moreover, it is well known that MPC polymers are biocompatible materials due to the relatively fewer protein-based interactions that occur at the tissue–implant interface [13–21, 28–30]. Thus, the use of MPC polymers offers interesting possibilities for obtaining injectable and biocompatible hydrogels [31–33].

Oligo(lactic acid) macromonomers were synthesized by a general method. Table 1 summarizes the polymerization results. The degree of polymerization of these macromonomers was approximately dependent on the feed ratio.

The polymerization of MPC and oligo(lactic acid) macromonomers proceeded homogeneously. The composition of each monomer unit in the MPC polymers corresponded to that in the feed monomer solution (Table 2). The polymers prepared using AIBN (A-PMLA) as the initiator did not dissolve but dispersed in water. On the other hand, the polymers formed by living radical polymerization using XDC (X-PMLA) as the iniferter were soluble in water (Scheme 2). The molecular weight distribution of A-PMLA was large. Small polymer particles dispersed in the aqueous medium may potentially cause inflammation and embolization. Therefore, A-PMLA was not suitable for application to medical materials. It is not entirely clear why the observed solubility of the polymers is different even if the MPC contents of the polymers are almost equal. However, one possible explanation may be the difference between the molecular weight distributions (M_n/M_w) of A-PMLA and X-PMLA. The M_n/M_w value of A-PMLA was larger than that of X-PMLA; thus, we could infer that A-PMLA included a water-insoluble portion due to its higher molecular weight. We considered that the molecular weight distribution of the polymer should be small in order to obtain stable hydrogels in an aqueous medium. Thus, we switched to the living radical polymerization method because using this method, we could regulate the M_n/M_w value. MPC polymers having 30 mol% MPC did not undergo biological reactions at the surface and thus showed excellent biocompatibility [15, 17, 29, 30]. The polymer used in this study contained approx. 90 mol% MPC, so we consider that this polymer has sufficient biocompatibility.

3.2. Effect of Polymer Concentration on Gelation Behavior

As shown in Fig. 2, spontaneous gelation occurred due to the mixing of aqueous solutions containing PMLLA and PMDLA, wherein the degree of polymerization of the oligo(lactic acid) macromonomer units was 12. The extent of gelation depended on the concentrations of both polymers, as summarized in Table 3. The lowest concentration required for gelation decreased with an increase in the molecular weight or the composition of oligo(lactic acid) macromonomer units. In previous studies, we investigated the formation of a stereocomplex between water-insoluble MPC polymers and enantiomeric poly(lactic acid) graft chains. Differential scanning calorimetry data and X-ray diffraction profiles of the precipitate from the polymer solution confirmed stereocomplex formation [11]. This suggests that the obtained

Table 2.
Synthesis of poly(MPC-graft-oligo(lactic acid))

Code	Macromonomer	Side-chain length	Monomer ratio in feed		Monomer unit composition in co-polymer[a]		Molecular weight ($\times 10^{-4}$)[b]	M_n/M_w[b]	Yield (%)	Water solubility[c]
			MPC	OL(D)LA	MPC	OL(D)LA				
A-PMLLA12-5	OLLA12	14	95	5	96	4	2.1	5.2	55	Turbid
A-PMLLA12-10	OLLA12	14	90	10	93	7	4.3	2.6	69	Turbid
A-PMLLA12-20	OLLA12	14	80	20	89	11	–	–	62	Turbid
A-PMLLA20-5	OLLA20	21	95	5	97	3	–	–	69	Turbid
A-PMLLA20-10	OLLA20	21	90	10	95	5	–	–	71	Turbid
A-PMLLA30-5	OLLA30	34	95	5	97	3	–	–	–	–
A-PMDLA12-5	ODLA12	13	95	5	95	5	–	–	59	Turbid
A-PMDLA12-10	ODLA12	13	90	10	93	7	–	–	66	Turbid
A-PMDLA12-20	ODLA12	13	80	20	88	12	–	–	48	Turbid
A-PMDLA20-5	ODLA20	19	95	5	97	3	2.7	2.4	85	Turbid
A-PMDLA20-10	ODLA20	19	90	10	94	6	–	–	83	Turbid
X-PMLLA20-5	OLLA12	20	95	5	97	3	1.6	2.0	64	Soluble
X-PMLLA20-10	OLLA12	20	90	10	93	7	2.4	1.7	–	Soluble
X-PMDLA20-5	ODLA12	20	95	5	96	4	2.7	2.4	–	Soluble
X-PMDLA20-10	ODLA12	20	90	10	92	8	2.1	1.4	–	Soluble

[a] Determined by ^{1}H-NMR.
[b] Determined with PEG standards.
[c] Concentration was 1 mg/ml.

Table 3.
Effect of polymer concentration on the gelation of A-PMLA and X-PMLA polymer systems

Code	L-polymer	D-polymer	Concentration of polymer (wt%)		
			5	10	20
SC12-5	A-PMLLA12-5	A-PMDLA12-5	Sol	Sol	Sol
SC12-10	A-PMLLA12-10	A-PMDLA12-10	Sol	Sol	Gel
SC12-20	A-PMLLA12-20	A-PMDLA12-20	Sol	Gel	Gel
SC20-5	A-PMLLA20-5	A-PMDLA20-5	Sol	Sol	Sol
SC20-10	A-PMLLA20-10	A-PMDLA20-10	Sol	Sol	Sol
X-SC20-5	X-PMLLA20-5	X-PMDLA20-5	Sol	Sol	Gel
X-SC20-10	X-PMLLA20-10	X-PMDLA20-10	Sol	Gel	Sol

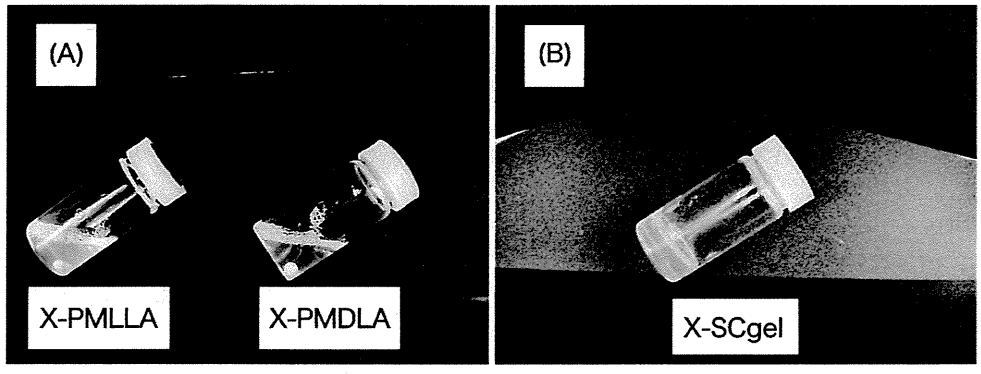

Figure 2. Pictures of gelation process resulting from the mixing of X-PMLLA and X-PMDLA (10 wt% aqueous solutions). (A) Aqueous solution of X-PMLLA20-10 (left) and X-PMDLA20-10 (right), (B) after mixing and standing for 24 h at room temperature.

hydrogel (X-SCgel) was produced by the formation of a stereocomplex between the L-form oligo(lactic acid) and the D-form oligo(lactic acid) as side-chains. On account of the hydrophobic nature of the oligo(lactic acid) side-chains, A-PMLA formed an aggregate in an aqueous medium. Therefore, it is necessary to organize the oligo(lactic acid) side-chains on the surface of the aggregate and for making easy interaction between these polymer chains. Oligo(lactic acid) macromonomers with 20 repeating lactic acid units had higher hydrophobicity than those with 12 repeating units, and the oligo(lactic acid) units were located inside the aggregate as cross-linking points. The gelation time of the X-SCgels depended on the polymer concentration. For instance, a mixture of 20 wt% polymers in the solution required 8.7 min for gelation, while a 15 wt% polymer solution required over 100 min (Fig. 3). Thus, we can control gelation time by changing polymer concentration.

3.3. Hydrolysis of the Hydrogel

The fluorescence intensity of the hydrogel containing PBS along with FITC-labeled BSA was measured to examine the degradation of the hydrogel. Since the perme-

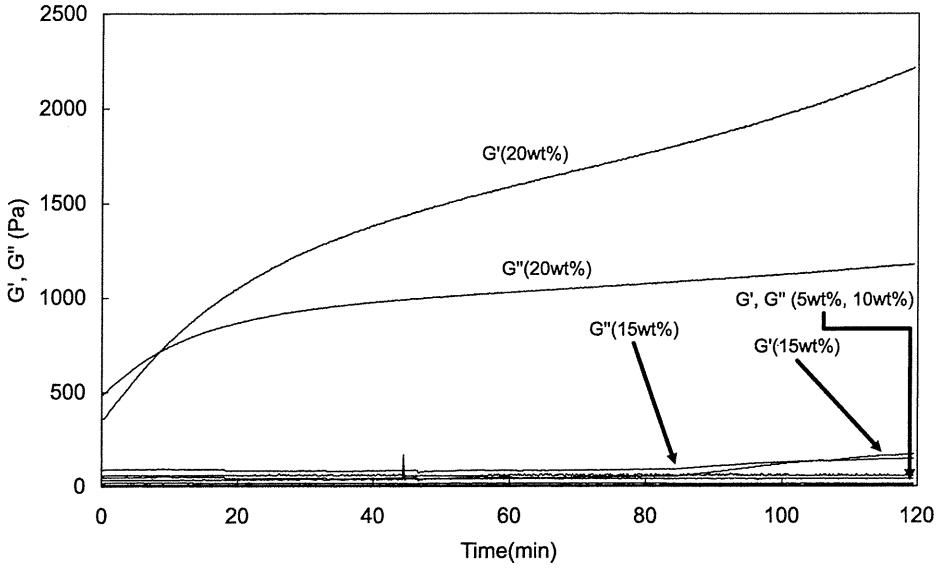

Figure 3. The elastic modulus (G') and viscous modulus (G'') of the mixture of X-PMLLA20-5 and X-PMDLA20-5 solutions with various concentrations.

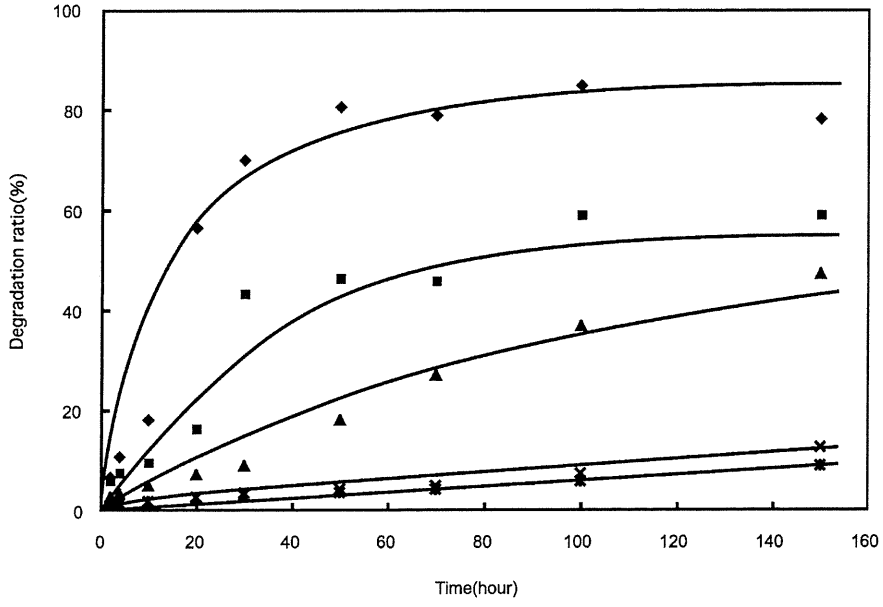

Figure 4. Degradation profile of X-SC gel (X-SC20-10) under various pH conditions. (◆) pH 7.8, (■) pH 7.4, (▲) pH 6.8, (×) pH 6.0 and (∗) pH 5.8.

ability of the hydrogel containing FITC-labeled BSA was substantially low due to the high molecular weight of BSA, the increase in fluorescence intensity almost corresponded to the degradation process of the hydrogel. In Fig. 4, the degrada-

tion ratio of the hydrogel, which is evaluated using the fluorescence intensity, is plotted as a function of time and pH. The fluorescence intensity became saturated at conditions corresponding to 100 h, 37°C and pH 7.4. The degradation rate increased in media with a higher pH. The X-SCgel disappeared in the PBS due to hydrolysis of oligo(lactic acid) chains and cross-linking points, which destroyed the stereocomplex. It could be suggested that the X-SCgel degrades under physiological conditions in the body. Furthermore, the main chains remained and were not degraded under physiological conditions; however, these chains are water-soluble polymers. The molecular weight of the main chain was controlled at less than 3.0×10^4. Thus, we consider that these chains can be excreted in urine. From an overall perspective, the results suggest that hydrogels composed of PMLLA and PMDLA can undergo hydrolysis under physiological conditions and that the products can be completely eliminated from the body.

4. Conclusion

To develop an injectable and biocompatible hydrogel system, we synthesized a water-soluble graft polymer composed of MPC and oligo(lactic acid) macromonomer units using living radical polymerization. These polymers underwent spontaneous gelation due to the formation of a stereocomplex between the racemates of oligo(lactic acid) macromonomer units in an aqueous medium. The properties of the hydrogel depended on the concentration of the polymers. The hydrogels degraded in a buffer solution by hydrolysis of the side chain, and the degradation products dissolved in the buffer solution. From these results, it is suggested that the polymer system could be applied as an injectable, biocompatible, and degradable hydrogel system to serve as a reservoir of bioactive molecules in drug-delivery systems and as a scaffold in cell-based tissue engineering.

Acknowledgements

The authors thank Associate Professor Tomohiro Konno, Dr. Ryosuke Matsuno and Dr. Yuuki Inoue, all from The University of Tokyo, for their valuable inputs. This study was partially supported by Core Research for Evolution Science and Technology (CREST), Japan Science and Technology Agency.

References

1. N. A. Peppas, *Hydrogels in Medicine and Pharmacy, Vol. III: Properties and Applications*. CRC Press, Boca Raton, FL (1987).
2. C. He, S. W. Kim and D. S. Lee, *J. Control. Rel.* **127**, 189 (2008).
3. A. Gutowska, B. Jeong and M. Jasionowski, *Anat. Rec.* **263**, 342 (2001).
4. S. J. de Jong, W. N. E. van Dijk-Wolthuis, J. J. Kettenes-van den Bosch, P. J. W. Schuyl and W. E. Hennink, *Macromolecules* **31**, 6397 (1998).
5. S. J. de Jong, S. C. De Smedt, M. W. C. Wahls, J. Demeester, J. J. Kettenes-van den Bosch and W. E. Hennink, *Macromolecules* **33**, 3680 (2000).

6. S. J. de Jong, B. van Eerdenbrugh, C. F. van Nostrum, J. J. Kettenes-van den Bosch and W. E. Hennink, *J. Control. Rel.* **71**, 261 (2001).
7. H. Tsuji, F. Horii, S. Hyon and Y.Ikada, *Macromolecules* **24**, 2719 (1991).
8. T. Fujiwara, T. Mukose, T. Yamaoka, H. Yamane, S. Sakurai and Y. Kimura, *Macromol. Biosci.* **1**, 204 (2001).
9. S. M. Li, A. El Ghzaoui and E. Dewinck, *Macromol. Symp.* **222**, 23 (2005).
10. S. M. Li and M. Vert, *Macromolecules* **36**, 8008 (2003).
11. J. Watanabe, T. Eriguchi and K. Ishihara, *Biomacromolecules* **3**, 1109 (2002).
12. J. Watanabe, T. Eriguchi and K. Ishihara, *Biomacromolecules* **3**, 1375 (2002).
13. K. Ishihara, R. Aragaki, T. Ueda, A. Watanabe and N. Nakabayashi, *J. Biomed. Mater. Res.* **24**, 1069 (1990).
14. K. Ishihara, N. P. Ziats, B. P. Tierney, N. Nakabayashi and J. M. Anderson, *J. Biomed. Mater. Res.* **25**, 1397 (1991).
15. K. Ishihara, H. Oshida, T. Ueda, Y. Endo, A. Watanabe and N. Nakabayashi, *J. Biomed. Mater. Res.* **26**, 1543 (1992).
16. K. Ishihara, T. Tsuji, Y. Sakai and N. Nakabayashi, *J. Polym. Sci. Part A: Polym. Chem.* **32**, 859 (1994).
17. K. Ishihara, H. Nomura, T. Mihara, K. Kurita, Y. Iwasaki and N. Nakabayashi, *J. Biomed. Mater. Res.* **39**, 323 (1998).
18. S. Sawada, S. Sakaki, Y. Iwasaki, N. Nakabayashi and K. Ishihara, *J. Biomed. Mater. Res. A* **64**, 411 (2003).
19. K. Ishihara, E. Ishikawa, A. Watanabe, Y. Iwasaki, K. Kurita and N. Nakabayashi, *J. Biomater. Sci. Polymer Edn* **10**, 1047 (1999).
20. S. Kihara, K. Yamazaki, K. N. Litwak, P. Litwak, M. V. Kameneva, H. Ushiyama, T. Tokuno, D. C. Borzelleca, M. Umeda, J. Tomioka, O. Tagusari, T. Akimoto, H. Koyanagi, H. Kurosawa, R. L. Kormos and B. P.Griffith, *Artif. Organs* **27**, 188 (2003).
21. M.Sakakida, K. Nishida, M. Shichiri, K. Ishihara and N. Nakabayashi, *Sensors Actuators* **13–14**, 319 (1993).
22. X. Xu, X. Chen, Z. Wang and X. Jing, *Eur. J. Pharm.* **72**, 18 (2009).
23. K. Hu, J. Li, Y. Shen, W. Lu, X. Gao, Q. Zhang and X. Jiang, *J. Control. Rel.* **134**, 55 (2009).
24. K. Ishihara, T. Ueda and N. Nakabayashi, *Polym. J.* **22**, 355 (1990).
25. T. Ueda, H. Oshida, K. Kurita, K. Ishihara and N. Nakabayashi, *Polym. J.* **24**, 1259 (1992).
26. T. Otsu and A. Kuriyama, *Polym. Bull.* **11**, 135 (1984).
27. D. W. Lim, S. Choi and T. G. Park, *Macromol. Rapid Commun.* **21**, 464 (2000).
28. A. L. Lewis, *Colloids Surface B: Biointerfaces* **18**, 261 (2000).
29. Y. Iwasaki and K. Ishihara, *Anal. Bioanal. Chem.* **381**, 534 (2005).
30. K. Ishihara and M. Takai, *J. Roy. Soc. Interface* **6** (Suppl.), S279 (2009).
31. T. Goda and K. Ishihara, *Expert. Rev. Med. Devices* **3**, 167 (2006).
32. M. Kimura, M. Takai and K. Ishihara, *J. Biomed. Mater. Res. A* **80**, 45 (2007).
33. M. Kimura, M. Takai and K. Ishihara, *J. Biomater. Sci. Polym. Edn* **18**, 623 (2007).

Biomaterials 32 (2011) 2241–2247

Contents lists available at ScienceDirect

Biomaterials

journal homepage: www.elsevier.com/locate/biomaterials

Tissue response to poly(L-lactic acid)-based blend with phospholipid polymer for biodegradable cardiovascular stents

Hyung Il Kim [a,b,h,i], Kazuhiko Ishihara [a,b,c,i,*], Seungbok Lee [d,e], Ji-Hun Seo [c,i], Hye Young Kim [f], Dongwhan Suh [d,e], Min Uk Kim [g], Tomohiro Konno [a,i], Madoka Takai [c], Jeong-Sun Seo [d,e,h,**]

[a] Department of Bioengineering, School of Engineering, The University of Tokyo, 7-3-1, Hongo, Bunkyo-ku, Tokyo 113-8656, Japan
[b] Center for Medical System Innovation, The University of Tokyo, Hongo, Bunkyo-ku, Tokyo 113-8656, Japan
[c] Department of Materials Engineering, School of Engineering, The University of Tokyo, Hongo, Bunkyo-ku, Tokyo 113-8656, Japan
[d] Department of Biomedical Sciences, Genomic Medicine Institute, Seoul National University College of Medicine, Seoul 110-799, Republic of Korea
[e] Department of Biochemistry and Molecular Biology, Genomic Medicine Institute, Seoul National University College of Medicine, Seoul 110-799, Republic of Korea
[f] Department of Anesthesiology and Pain Medicine, Seoul National University Hospital, Seoul 110-744, Republic of Korea
[g] Department of Radiology, Seoul National University Hospital, Seoul 110-744, Republic of Korea
[h] Macrogen Inc., Seoul 153-023, Republic of Korea
[i] Core Research for Evolutional Science and Technology (CREST), Japan Science and Technology Agency, 5 Sanban-cho, Chiyoda-ku, Tokyo 102-0075, Japan

ARTICLE INFO

Article history:
Received 28 September 2010
Accepted 27 November 2010
Available online 24 December 2010

Keywords:
Polymer blend
poly(lactic acid)
Phosphorylcholine group
Tissue compatibility
Cardiovascular stent

ABSTRACT

A temporary cardiovascular stent device by bioabsorbable materials might reduce late stent thrombosis. A water-soluble amphiphilic phospholipid polymer bearing phosphorylcholine groups (PMB30W) was blended with a high-molecular-weight poly(L-lactic acid) (PLLA) to reduce unfavorable tissue responses at the surface. The PLLA implants and the polymer blend (PLLA/PMB30W) implants were inserted into subcutaneous tissues of rats, the infrarenal aorta of rats, and the internal carotid arteries of rabbits. After 6 months subcutaneous implantation, the PLLA/PMB30W maintained high density of phosphorylcholine groups on the surface without a significant bioabsorption. After intravascular implantation, the cross-sectional areas of polymer tubing with diameters less than 1.6 mm were histomorphometrically measured. Compared to the PLLA tubing, the PLLA/PMB30W tubing significantly reduced the thrombus formation during 30 d of implantation. Human peripheral blood mononuclear cells were cultured on the PLLA and the PLLA/PMB30W to compare inflammatory reactions. Enzyme-linked immunosorbent assay quantified substantially decreased proinflammatory cytokines in the case of the PLLA/PMB30W. They were almost the same level as the negative controls. Thus, we conclude that the phosphorylcholine groups could reduce tissue responses significantly both in vivo and in vitro, and the PLLA/PMB30W is a promising material for preparing temporary cardiovascular stent devices.

1. Introduction

The treatment of coronary artery disease and other cardiovascular diseases has been revolutionized through the introduction of interventional procedures and the use of intravascular stents, which are inserted by a minimally invasive method and mechanically scaffold the vessel wall against elastic recoil, improving blood flow in diseased vessels [1,2]. However, current drug-eluting stents permanently remain in implantation sites with several limitations, including the risks of late stent thrombosis, hindrance of late lumen vessel enlargement, and interference with radiological imaging [3]. High-molecular-weight poly(L-lactic acid) (PLLA) has the potential to replace permanent stenting and has exhibited favorable degradation behavior in small clinical trials [3–5]. The PLLA is a biodegradable polymer whose molecular weight decreases over time due to cleavage of the ester linkage, degrading into small particles that can be phagocytosed [3,4]. Eventually, the PLLA is degraded into lactic acid and is eliminated through the citric acid cycle.

Safety concerns regarding the use of the PLLA for stenting remain, however, because foreign materials are inherently

* Corresponding author. Department of Bioengineering, School of Engineering, University of Tokyo, Tokyo 113-8656, Japan. Tel.: +81 3 5841 7124; fax: +81 3 5841 8647.
** Corresponding author. Department of Biomedical Sciences, Genomic Medicine Institute, Seoul National University College of Medicine, Seoul 110-799, Republic of Korea. Tel.: +82 2 740 8246; fax: +82 2 741 5423.
E-mail addresses: ishihara@mpc.t.u-tokyo.ac.jp (K. Ishihara), jeongsun@snu.ac.kr (J.-S. Seo).

0142-9612/$ – see front matter © 2010 Elsevier Ltd. All rights reserved.
doi:10.1016/j.biomaterials.2010.11.067

thrombogenic [6–11]. This is attributed to the denaturation of proteins, activation of coagulation factors, propagation of thrombi, provocation of inflammatory responses, and accumulation of debris. To control these adverse tissue reactions on the materials, the surface of the materials was covered with phosphorylcholine groups for preparing artificial cell membrane without any ligand molecules. Based on this hypothesis, 2-methacryloyloxyethyl phosphorylcholine (MPC) copolymers, which have phosphorylcholine groups in their side chain, have been synthesized [12–17]. The MPC copolymers can be incorporated by a convenient procedure such as blending with matrix polymers [18–21]. In a molecular and mechanistic approach, the biomedical function of the MPC copolymers has been explained by the free water fraction on the surface, which minimizes protein adsorption and its conformational change [22–24]. Surfaces of materials with a high density of phosphorylcholine groups significantly lower platelet activation and neointimal hyperplasia [25–30]. A water-soluble poly[MPC-*co*-*n*-butyl methacrylate (BMA)] (PMB30W) is an amphiphilic copolymer composed of hydrophobic BMA units and hydrophilic MPC units [12,13,31]. Due to its strong amphiphilic characteristics, the PMB30W plays a dual role as a biomimetic modifier of surface properties and as a surfactant for the bulk properties of polymer blends composed of PLLA and PMB30W (PLLA/PMB30W) [11].

Although it has been presumed that phosphorylcholine groups on the surface of materials can enhance biocompatibility, the critical concept that the incorporation of phosphorylcholine groups might reduce stent thrombosis has not been resolved in vitro [32], preclinically [33], or clinically [34]. This discrepancy may be due to the different dispersion state of phosphorylcholine groups on the surfaces of stent materials [11,14–17,32,33]. In the present study, we hypothesized that the PLLA/PMB30W with phosphorylcholine group-rich surfaces could exhibit favorable bulk and surface properties in vivo and may enhance tissue compatibility of temporary cardiovascular stent devices. Therefore, the objective of this study was comparison of tissue responses on the PLLA/PMB30W and the PLLA in vivo with small animal models and in vitro, and to discuss the role of the phosphorylcholine groups for reducing the tissue responses.

2. Materials and methods

2.1. Preparation of materials

The PLLA (molecular weight (Mw) = 1×10^5 for the preparation of tubing or Mw = 5×10^4 for the preparation of films) was purchased from Polysciences, Warrington, PA. The PMB30W was synthesized using a free radical polymerization technique by a previously reported method [12,13,31]. The chemical structure of PMB30W is shown in Fig. 1. The PMB30W concentrations >1 mg/mL in phosphate-buffered saline (PBS) result in the PMB30W nanoaggregates with hydrodynamic diameters <20 nm [31,35].

The PLLA and the PLLA/PMB30W (weight ratio, 92/8) tubing and films were prepared by a modified previously reported method [11]. Briefly, 6 wt% PLLA solution in dichloromethane (DCM)/methanol (MeOH) (volume ratio, 12/1) and 6 wt% PLLA/PMB30W (weight ratio, 92/8) solution in DCM/MeOH (volume ratio, 12/1) were repeatedly coated onto Teflon® rods (tubing) or cast onto Teflon® dishes (films), and the solvents were dried at room temperature. Polymer tubing and films were vacuum-dried for 1 week, and then immersed in water to equilibrate the surface overnight before the surface measurements. Polymer tubing and films were sterilized with ethylene oxide gas at 40 °C.

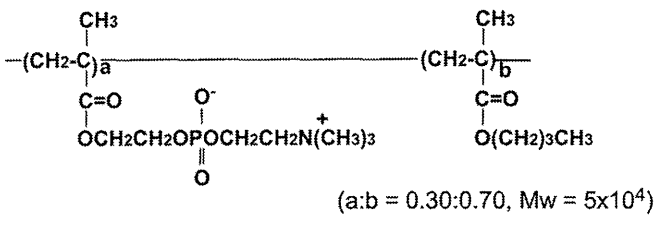

Fig. 1. The chemical structure of the PMB30W.

2.2. Surface characteristics of materials

To analyze the inner surface of polymer implants, the tubing was cut into concave membranes and pressed under 50 MPa at 60 °C for 10 min. The atomic concentration on the inner surface was measured using an X-ray photoelectron spectroscope (XPS; AXIS-HSi, Kratos/Shimadzu, Kyoto, Japan) with a magnesium Kα (energy = 1253.6 eV) source radiation. The photoelectron take-off angle was 90°. The measured phosphorous atomic concentration was attributed to the phosphorus in the phosphorylcholine groups of the PMB30W. The phosphorous/carbon atomic concentration ratios (P/C% values) were calculated by determining the relevant integral peak area and applying the sensitivity factors supplied by the instrument manufacturer (Supplementary Fig. 1).

To measure the static contact angle (SCA), a captive-bubble method was used. The polymer films were fixed horizontally, and a small air bubble was attached to the mold contact surface of polymer films in the distilled water and the SCA in water was determined by the angle between the films and the air bubble using a contact angle goniometer (CA-W, Kyowa, Saitama, Tokyo, Japan) at room temperature.

2.3. Evaluation of bioabsorption of polymer implants after subcutaneous implantation

Animal care and procedures were approved by Institutional Animal Care and Use Committee (IACUC) (No. 080929-3) at Seoul National University. The PLLA (n = 15) and PLLA/PMB30W (n = 15) polymer tubing (internal diameter [ID]: 1.6 mm; thickness: 0.2 mm; length: 2.5 cm) was implanted into the interscapular subcutaneous tissue of rats (n = 30, male Wistar, body weight: 0.3–0.4 kg) after anesthesia by inhalation of 2% isoflurane. At predetermined times (2, 4, 6 months), the polymer tubing was explanted after the animals were euthanized. The fibrous capsule surrounding the tubing was carefully removed. The polymer tubing was sonicated in 1% sodium dodecyl sulfate aqueous solution for 20 min to remove the adsorbed components and rinsed with distilled water. After vacuum drying, changes in the overall mass and molecular weight of the polymer tubing were calculated by a gravimetric method and gel permeation chromatography (Jasco system, Tokyo, Japan), respectively. The polymer tubing was dissolved in 1,1,1,3,3,3-hexafluoroisopropanol; the flow was 0.2 mL/min at 40 °C. The molecular weight of polymer was calibrated by poly(methyl methacrylate) standards.

2.4. Evaluation of acute thrombus formation after intravascular tubing insertion into small animals

Animal care and procedures were approved by IACUC (No. 08-0266) at Seoul National University Hospital.

Wistar male rats (n = 17, body weight: 0.3–0.4 kg) were anesthetized by inhalation of 2% isoflurane. After the infrarenal abdominal aorta of each animal was surgically exposed and clipped by an approximator with a surgical microscope, the vessels were carefully punctured using a taper-point needle. Then, polymer tubing (n = 17; ID: 1.2 mm; thickness: 150 μm; length: 2.0 mm) was inserted using a 20 G catheter, and the puncture sites were sutured with Ethilon 10-0 as described in Results.

For paired tests, New Zealand white male rabbits (n = 11, body weight: 3–4 kg) were anesthetized by intramuscular injection of a mixture of Zoletil (15 mg/kg) and xylazine (7.5 mg/kg) and subsequent inhalation of nitric oxide and isoflurane. Heparin (50 IU/kg per h) was administered to the rabbits as a continuous infusion during the operative procedure. With a surgical microscope, each internal carotid artery was carefully exposed and clipped by an approximator. After puncturing vessels by the aforementioned method, the polymer tubing (n = 22; ID: 1.6 mm; thickness: 150 μm; length: 3.0 mm) was inserted using an 18 G catheter. The PLLA tubing (n = 11) was inserted into the left internal carotid arteries, and the PLLA/PMB30W tubing (n = 11) was inserted into the right internal carotid arteries. The puncture sites were then sutured with Ethilon 8-0.

At predetermined times (3 h and 30 d in the rat study; 2 d and 30 d in the rabbit study), the polymer tubing-inserted arteries were surgically explanted after a heparin injection (200 IU/kg), following which the animals were euthanized. The samples were then rinsed with normal saline, placed in 2.5% glutaraldehyde PBS solution overnight, rinsed with distilled water, embedded in optimal cutting temperature compound, and cross-sectioned (thickness: 0.30 mm) while in a deep frozen state. The frozen sections were prepared by an independent researcher. For morphometric analysis, all cross-sections [PLLA from rats at 3 h (n = 13), PLLA/PMB30W from rats at 3 h (n = 12), PLLA from rats at 30 d (n = 8), PLLA/PMB30W from rats at 30 d (n = 10), PLLA from rabbits at 2 d (n = 26), PLLA/PMB30W from rabbits at 2 d (n = 20), PLLA from rabbits at 30 d (n = 32), PLLA/PMB30W from rabbits at 30 d (n = 29)] were digitally exported from a microscope camera, and the patent cross-sectional area (CSA) was analyzed using the National Institutes of Health ImageJ software (version 1.41o). Lumen area stenosis (LAS) was calculated as $[1.00 - (S/T)] \times 100$, where T is the CSA of the unimplanted polymer tubing, and S is the minimal CSA of each polymer tubing-inserted artery. In the rat study, T = 1.13 mm^2, and in the rabbit study, T = 2.01 mm^2. For observation of vessel remodeling, a PLLA/PMB30W-inserted aorta of rat (n = 1) after 50 d of implantation

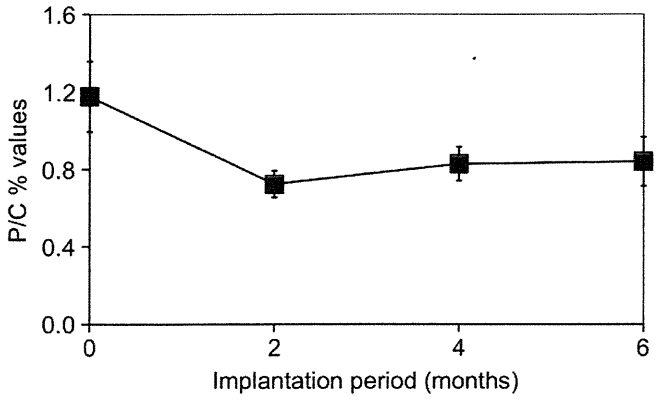

Fig. 2. Surface characteristics of the PLLA/PMB30W over 6 months of subcutaneous implantation. The P/C% values of the inner surface of the PLLA/PMB30W tubing (n = 4–5 implants per time point) were measured by X-ray photoelectron spectroscopy.

was embedded with acrylic resin. The cross-sections were prepared by a standard microtome and stained with hematoxylin-eosin.

2.5. Evaluation of proinflammatory cytokines released form human peripheral blood mononuclear cells during contact with polymer films

Human peripheral blood mononuclear cells (hPBMCs) from a single healthy donor were purchased from Lonza (Basel, Switzerland). The hPBMCs were incubated in RPMI-1600 with 10% FBS, 100 units/mL penicillin, 100 μg/mL streptomycin, 2 mM glutamine, 40 units/mL DNase, and 70 ng/mL G-CSF on commercially available 12-well polystyrene plates treated with an MPC polymer (Nunc Japan, Tokyo, Japan) with and without the PLLA or the PLLA/PMB30W films (diameter: 20 mm, thickness: 0.2 mm) at densities of 2.0×10^6 hPBMCs per well. The mold contact surface of polymer films was placed upward. At 24 h, supernatants were collected after centrifugation at 200 × g for 15 min. Then, the hPBMCs were incubated in fresh medium. The supernatants were collected 48 h after centrifugation at 200 × g for 15 min. Commercially available kits based on the enzyme-linked immunosorbent assay (ELISA) (R&D Systems, Minneapolis, MN) were employed for the quantitative determination of macrophage migration inhibitory factor (MIF), monocyte chemoattractant protein-1 (MCP-1), interleukin 1β (IL-1β), IL-6, and tumor necrosis factor-α (TNF-α). Each standard and sample was tested in duplicate; samples that have a variation coefficient >0.20 were remeasured. The absorbance of each sample was recorded using a microplate reader after the blank subtraction that corrects optical imperfections in the plate.

2.6. Statistical analysis

Data are expressed as means and standard deviations. Statistical differences ($^*P < 0.05$; $^{**}P < 0.01$; $^{***}P < 0.001$) were analyzed by the Mann–Whitney U test for the animal studies and the analysis of variance (ANOVA) with the Bonferroni correction for the in vitro study.

3. Results and discussion

3.1. Bioabsorption of polymer implants after subcutaneous implantation

The subcutaneous milieu is considered adequate for evaluation of the basic properties of cardiovascular implants, such as biodegradation [36]. Rapid biodegradation of temporary stent materials could lead to incomplete opposition to vessel recoil forces [3–5]. Over the 6-month observation period, weight loss of both PLLA and PLLA/PMB30W was about 2% and the average molecular weight of the PLLA and that of the PLLA/PMB30W still remained over 93% of the initial values (Supplementary Fig. 2). During biodegradation, the changing molecular weight of the PLLA precedes its mass change and determines its bulk properties [11,37]. Because the molecular weight of the PLLA and the PLLA/PMB30W was not changed substantially, it is assumed that the mechanical strengths of the PLLA or those of the PLLA/PMB30W remain unaltered over 6 months of subcutaneous implantation.

The PMB30W is a water-soluble polymer and can be eluted from the surface of implants. However, we previously demonstrated that the tightly entangled blend system of the PLLA/PMB30W did not exhibit a substantial loss of the PMB30W on the surface of tubing during PBS incubation [11]. Fig. 2 shows that the density of phosphorylcholine groups on the inner surface of the PLLA/PMB30W eventually approached equilibrium (the P/C% values = 0.8 ± 0.1) between hydrophilic attraction from the in vivo environment and hydrophobic molecular entanglement with the PLLA chains. These results suggest that the PLLA/PMB30W maintained stable bulk and surface properties during 6 months implantation in vivo.

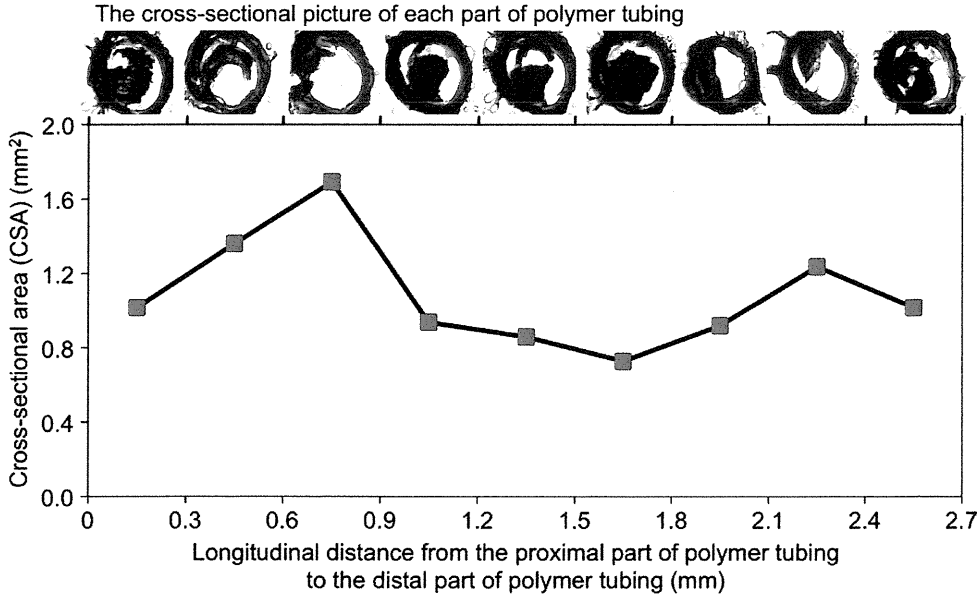

Fig. 3. Analysis of the cross-sectional areas (CSA) of the PLLA/PMB30W tubing after 30 d implantation into an internal carotid artery of a rabbit. After the explanation of the polymer tubing, they were cross-sectioned (thickness: 0.30 mm) while in a deep frozen state. For morphometric analysis, all cross-sections were digitally exported from a microscope camera as shown in the above the figure, and the CSA was calculated using the National Institutes of Health ImageJ software.

Table 1
Cross-sectional areas (CSA) of polymer tubing after implantation into the infrarenal aorta of rats. The CSA of the unimplanted polymer tubing (T) was 1.13 mm^2.

	Number of implants	Implantation period	Mean CSA (mm^2)	Minimal CSA (S) (mm^2)	Lumen area stenosis (%) [{1.00 − (S/T)} × 100]
PLLA	3	3 h	0.14 ± 0.05	0.05 ± 0.05	95.7 ± 4.5
PLLA/PMB30W	3	3 h	0.48 ± 0.03	0.30 ± 0.14	73.3 ± 13.7
PLLA	3	30 d	0.27 ± 0.12	0.23 ± 0.14	79.3 ± 12.5
PLLA/PMB30W	4	30 d	0.66 ± 0.27	0.48 ± 0.20	61.6 ± 21.4

3.2. Acute thrombus formation after intravascular tubing insertion

The procedure of intravascular tubing insertion into small animals has been employed and modified for the evaluation of blood clot formation on the polymer tubing [38]. Because the diameter of the tubing was larger than that of the arteries in which they were implanted and the tubing fully covered the vessel lumen (Supplementary Fig. 3), incomplete apposition was not observed. All polymer implants had identical morphology; any thrombus in the implanted arteries was deposited on the surface of the materials, and CSAs of polymer tubing represent the patent lumen areas as shown in Fig. 3. In our animal models, the vessel wall, which is a compartment rich in tissue factors, was disrupted by puncturing the vessels. Simultaneously, exposed collagen and foreign materials triggered the accumulation and activation of platelets [9]. To focus on material-associated thrombosis, no antithrombotics, except heparin, were administered to the animals. Thus, thrombi were rapidly formed and propagated into the polymer implants, of which the distal part was located approximately 2 mm proximal to the puncture site. This rapid and extensive thrombus formation in small-diameter (<2 mm) vessels can be correlated with frequent failure of small-diameter (<6 mm) vascular prostheses.

Three out of 10 rats in the 30 d groups (PLLA at 1 d, PLLA at 3 d, PLLA/PMB30W at 1 d) died following bilateral lower extremity paralysis due to the occlusion of abdominal aorta and were excluded from further comparisons (Supplementary Fig. 4). Table 1 shows the unpaired comparison of the CSA of the lumens of the PLLA versus those of the PLLA/PMB30W tubing after implantation into the infrarenal aorta of rats. At 3 h after implantation, the averages of mean and minimal CSA of the PLLA versus the PLLA/PMB30W tubing were 0.14 mm^2 versus 0.48 mm^2 and 0.05 mm^2 versus 0.30 mm^2, respectively. At 30 d after implantation, the corresponding values were 0.27 mm^2 versus 0.66 mm^2 and 0.23 mm^2 versus 0.48 mm^2, respectively.

One out of 5 rabbits in the 2 d group was euthanized because the animal was unable to move and suffered from loss of brain function after the surgery. Additionally, 1 out of 6 rabbits in the 30 d group was diagnosed with an infection and euthanized. Table 2 shows the paired comparison of the CSAs of the PLLA versus the PLLA/PMB30W tubing after the materials were implanted into the internal carotid arteries of the rabbits. At 2 d after implantation, the averages of mean and minimal CSA of the PLLA versus the PLLA/PMB30W tubing were 0.38 mm^2 versus 0.88 mm^2 and 0.15 mm^2 versus 0.55 mm^2, respectively. At 30 d, the corresponding values were 0.55 mm^2 versus 0.93 mm^2 and 0.26 mm^2 versus 0.66 mm^2, respectively.

The averages of the total CSA (CSAs overall of the cross-sections) of the PLLA versus the PLLA/PMB30W after implantation into infrarenal aorta of rats were 0.18 mm^2 ($n = 13$) versus 0.49 mm^2 ($n = 12$) ($P = 0.0002$) at 3 h and 0.24 mm^2 ($n = 8$) versus 0.67 mm^2 ($n = 10$) ($P = 0.0019$) at 30 d (Fig. 4A). The corresponding values after implantation into internal carotid artery of rabbits were 0.37 mm^2 ($n = 26$) versus 0.84 mm^2 ($n = 20$) ($P < 0.0001$) at 2 d and 0.59 mm^2 ($n = 32$) versus 0.96 mm^2 ($n = 29$) ($P < 0.0001$) at 30 d (Fig. 4B).

Considering that thrombosis was initiated in vulnerable areas, thrombus propagation on the stent materials would depend on platelet deposition, accumulation of tissue factors, and generation of fibrin [9,10]. The surfaces containing high density of phosphorylcholine groups have the free water fraction and could reduce the thrombus formation [22–24]. During the remodeling process, the thrombus slowly regressed over time. The remaining thrombus volume provided a provisional matrix [7] into which smooth muscle cells migrated, proliferated, and synthesized extracellular matrix (Fig. 5). The remarkable thrombus formation on polymer implants was presumably due to the short distance (~2 mm) between the puncture site and the implantation site. Further, no antithrombotics (except heparin in the rabbit study) were administered, which is different from the real clinical situation. Thus, significantly different levels of thrombus formation were observed between the PLLA and the PLLA/PMB30W.

Intravascular tubing insertion has several merits for the exploration of blood-stent material interactions; a uniformly circular lumen shape of stent materials could control vascular responses [39], and CSA can be obtained by simple objective histomorphometry. In contrast, in vitro tests of thrombogenicity hinder the full range of interactions among platelets, complementary systems, and cellular components and produce inevitable artifacts of the blood–air interaction and of blood with other substrates; such systems are thus generally incapable of predicting in vivo performance [40]. In the present study, the in vivo inflammatory reaction has not been compared because the polymers showed brittleness on a standard microtome and elongation in the acrylic resin embedding. Moreover, the mechanical injury caused by the rigid scaffolds and surgical procedures could mask the inflammatory reaction of tissues contacting materials in both subcutaneous and intravascular implantation. For these reasons, thick frozen cross-sections (thickness: 0.30 mm) were primarily prepared for histomorphometric measurements (See Fig. 3).

3.3. Proinflammatory cytokines released form human peripheral blood mononuclear cells during contact with polymer films

Although thrombus formation and the inflammatory reaction are interconnected [40–42], inflammation without acute thrombosis

Table 2
Cross-sectional areas (CSA) of polymer tubing after implantation into the internal carotid arteries of rabbits. The CSA of the unimplanted polymer tubing (T) was 2.01 mm^2.

	Number of implants	Implantation period	Mean CSA (mm^2)	Minimal CSA (S) (mm^2)	Lumen area stenosis (%) [{1.00 − (S/T)} × 100]
PLLA	4	2 d	0.38 ± 0.08	0.15 ± 0.11	92.3 ± 5.4
PLLA/PMB30W	4	2 d	0.88 ± 0.41	0.55 ± 0.30	72.8 ± 15.0
PLLA	5	30 d	0.55 ± 0.28	0.26 ± 0.11	87.1 ± 5.7
PLLA/PMB30W	5	30 d	0.93 ± 0.16	0.66 ± 0.19	67.2 ± 9.2

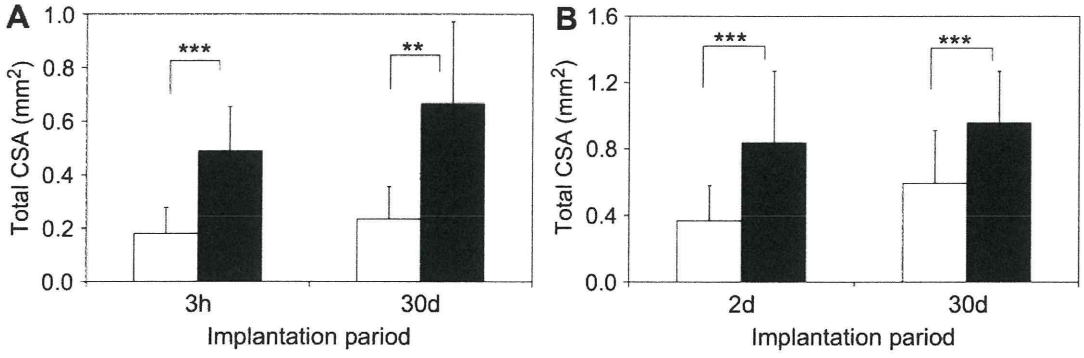

Fig. 4. Comparison studies of the CSA in the PLLA (open column) and the PLLA/PMB30W (closed column) after intravascular implantation into (A) the infrarenal aorta of rats and (B) the internal carotid arteries of rabbits. The *P* values were obtained by the Mann–Whitney *U* test.

can occur and trigger restenosis. Since acute thrombosis has been reduced by the evolution of surgical procedures and antithrombotics, chemokines expressed from a variety of cells, such as neutrophils and monocytes, have become more relevant to the chronic responses toward biomaterials [41]. Thus, inflammatory cytokines of hPBMCs were evaluated after contact with the PLLA films, the PLLA/PMB30W films, or no-polymer films.

The PLLA/PMB30W films have a moderately hydrophilic surface (SCA = 35 ± 8°), while the PLLA films are hydrophobic (SCA = 61 ± 8°). Because hydrophilic phosphorylcholine groups may rearrange at the water interface in an aqueous environment, a captive-bubble method was employed to determine SCA. The P/C % values of the mold contact surface of the PLLA/PMB30W films reached 1.33 after overnight incubation in water.

Fig. 6 shows concentrations of proinflammatory cytokines from hPBMCs cultured with and without polymer films. (The numerical data are available in Supplementary Table 1.) The MIF is considered to be a key player in the inflammatory reaction and in cardiovascular disease, and may play a proximal role in the hierarchy of cytokines [43]. Monocytes play a critical role in defense against foreign organisms and in regulating the behavior of other cells. The MCP-1 is thought to be responsible for monocyte recruitment in acute and chronic inflammation [44]. The acute phase cytokines IL-1β, IL-6, and TNF-α are produced early during inflammatory processes in cardiovascular tissue [45]. Thus, MIF, MCP-1, IL-1β, IL-6, and TNF-α in hPBMCs were quantified after contact with materials.

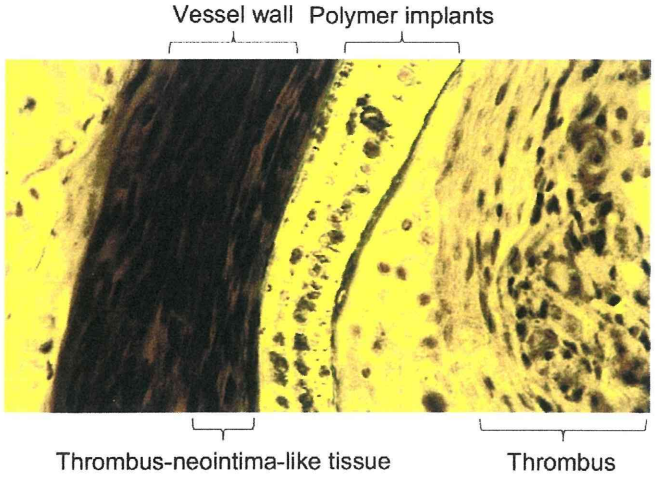

Fig. 5. A vessel remodeling after the intravascular tubing insertion. A cross-section of the polymer tubing-inserted artery at 50 d shows thrombus-neointima-like tissues leading to apposition of polymer implants, and the thrombus remained on the inner surface of the polymer implant. The polymer was elongated during embedding with acrylic resin. Smooth muscle cells proliferated into the thrombotic matrix.

Compared to the PLLA, the PLLA/PMB30W stimulated less robust proinflammatory cytokine activation. Although high concentrations of the MIF were observed in all groups at 1 d, the MIF concentrations were lowest on the no-polymer film (negative control) and were highest on the PLLA at 3 d. The high MIF expression observed at 1 d could be due to the freezing and thawing of hPBMCs before contact with the materials. At 1 d, both the PLLA and the no-polymer film induced high concentrations of MCP-1 compared with that induced by the PLLA/PMB30W. At 3 d, the no-polymer film amplified MCP-1 production while the PLLA and the PLLA/PMB30W did not. The amplification of MCP-1 production on the no-polymer film can be explained as a danger signal for surviving monocytes. Hydrophilic substrates increase the proportion of adherent apoptotic monocytes/macrophages [46], and hydrophilic phosphorylcholine groups contribute to suppressing monocyte adhesion on the surfaces of materials [47,48]. However, the generation of cytokines by monocytes is not proportional to the number of cells adherent to the surface [49]. Here, high MCP-1 expression represents a double-edged survival strategy, protecting cells from apoptosis and enabling them to migrate toward targets [50]. In an optical examination, clustered hPBMCs were observed on no-polymer film, but not on polymer film. This suggests that the cell–cell interaction was far more significant on extremely hydrophilic substrates [51]. Although it is clear that the lowest expression of MCP-1 on the PLLA/PMB30W films indicates monocyte quiescence, this may be interpreted with caution, when compared to the no-polymer film. In vivo, monocytes have a universal chance to migrate toward other sites unlike in vitro culture, where the cells make permanent contact with the hydrophilic surface and confront hydrophilic apoptosis. Concentrations of IL-1β and IL-6 were substantially different on the PLLA and the PLLA/PMB30W at 1 d. At 3 d, concentrations of IL-1β and IL-6 on the PLLA/PMB30W and on the no-polymer film were below detection limits, while those on the PLLA were increased (data not shown). The release of TNF-α stimulated by the PLLA and the PLLA/PMB30W was significantly different at 1 and 3 d. Relatively high expression of TNF-α could be due to administration of G-CSF into the culture medium, although other reports have previously described discrepancies in the expression of TNF-α and IL-1β by hPBMCs [52]. The mechanism that evokes the inflammatory reaction of hPBMCs to biomaterials has yet to be elucidated [41]. Monocyte inactivation on hydrophilic substrates prevents differentiation of macrophages [46], but the apoptosis of healthy monocytes does not guarantee cytocompatibility.

The surfaces covered with phosphorylcholine groups significantly improved cytocompatibility [18,47,48,53] by modulating the

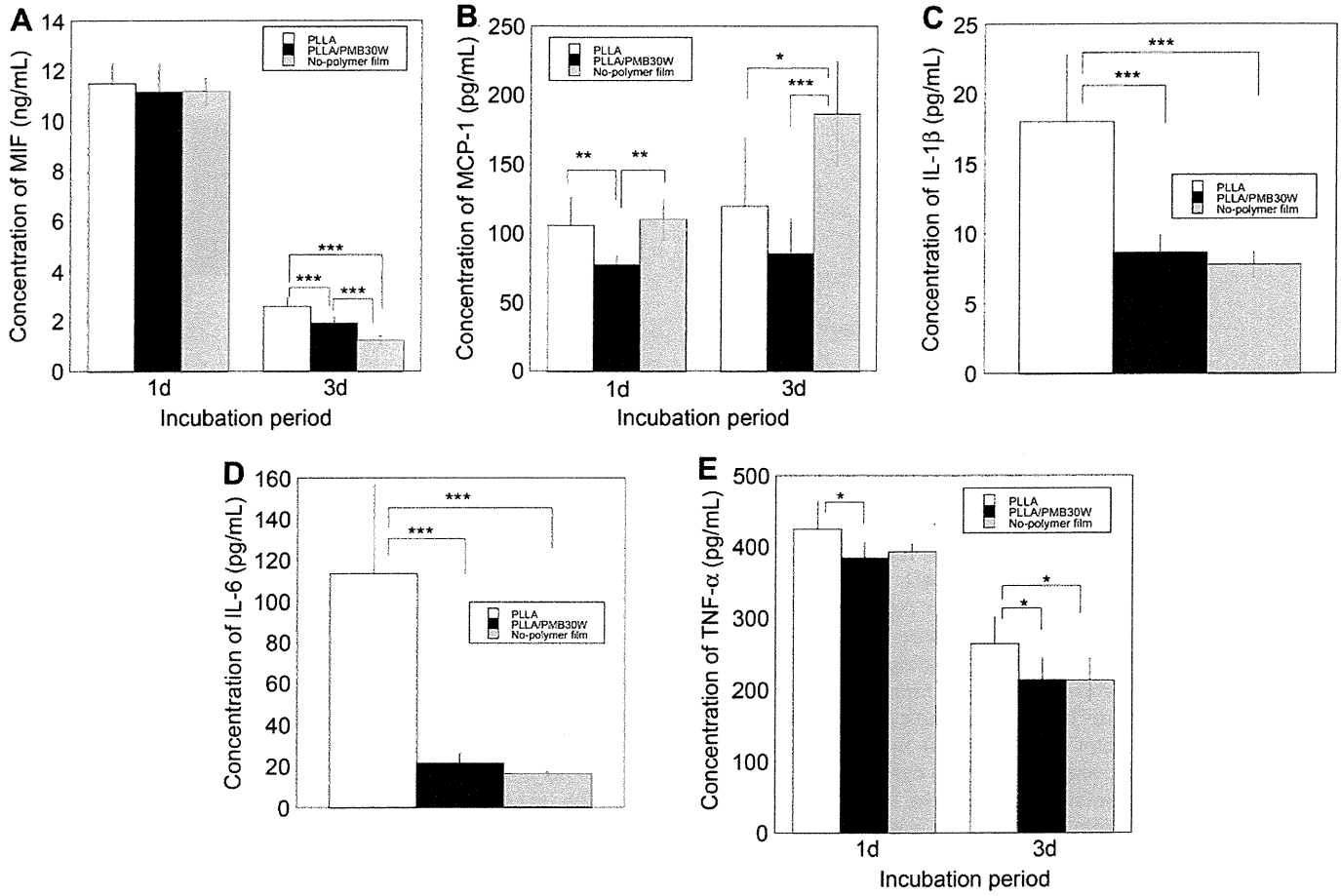

Fig. 6. Inflammatory cytokines released by human peripheral blood mononuclear cells. Data are presented as 8 cultures (PLLA and PLLA/PMB30W) and 7 cultures (No-polymer film). (A) MIF = macrophage migration inhibitory factor; (B) MCP-1 = monocyte chemoattractant protein-1; (C) IL-1β = interleukin 1β at 1 d; (D) IL-6 = interleukin 6 at 1 d; (E) TNF-α = tumor necrosis factor α. The *P* values were obtained by ANOVA with the Bonferroni correction.

leukocyte-mediated inflammatory reaction with monocyte quiescence. These findings strongly suggest that the homeostasis of human blood cells can be maintained by phosphorylcholine groups located on the surface of temporary cardiovascular stent materials.

4. Conclusion

Adverse tissue responses toward the PLLA used for temporary stenting were significantly reduced when the surface of the PLLA was covered with the phosphorylcholine groups by simple blending with an amphiphilic MPC copolymer, the PMB30W. In addition to temporary stenting eliminating the safety concerns involved in permanent cardiovascular stenting, the PLLA/PMB30W could reduce thrombotic occlusion under in vivo models and inflammatory reactions in vitro model. Therefore, we can believe that the PLLA/PMB30W is a promising material for temporary cardiovascular stent. A further investigation based on interventional procedures in large animal studies with long-term follow-up is necessary to confirm the clinical utility of these materials.

Acknowledgement

The authors are grateful for the helpful discussion and advice provided by Prof. Ung-Il Chung (The University of Tokyo). The assistance of the Global COE program in CMSI supported by the MEXT in Japan is acknowledged.

Appendix

Figures with essential color discrimination. Figs. 3 and 5 in this article are difficult to interpret in black and white. The full color images can be found in the online version, at doi:10.1016/j.biomaterials.2010.11.067.

Appendix. Supplementary data

Supplementary data associated with article can be found in online version at doi:10.1016/j.biomaterials.2010.11.067.

References

[1] Serruys PW, Kutryk MJ, Ong AT. Coronary-artery stents. N Engl J Med 2006;354:483–95.
[2] Mueller RL, Sanborn TA. The history of interventional cardiology: cardiac catheterization, angioplasty, and related interventions. Am Heart J 1995;129:146–72.
[3] Serruys PW, Ormiston JA, Onuma Y, Regar E, Gonzalo N, Garcia-Garcia HM, et al. A bioabsorbable everolimus-eluting coronary stent system (ABSORB): 2-year outcomes and results from multiple imaging methods. Lancet 2009;373:897–910.
[4] Ormiston JA, Serruys PW, Regar E, Dudek D, Thuesen L, Webster MW, et al. A bioabsorbable everolimus-eluting coronary stent system for patients with single de-novo coronary artery lesions (ABSORB): a prospective open-label trial. Lancet 2008;371:899–907.
[5] Tamai H, Igaki K, Kyo E, Kosuga K, Kawashima A, Matsui S, et al. Initial and 6-month results of biodegradable poly-l-lactic acid coronary stents in humans. Circulation 2000;102:399–404.

[6] van der Giessen WJ, Lincoff AM, Schwartz RS, van Beusekom HM, Serruys PW, Holmes Jr DR, et al. Marked inflammatory sequelae to implantation of biodegradable and nonbiodegradable polymers in porcine coronary arteries. Circulation 1996;94:1690–7.
[7] Schwartz RS, Holmes Jr DR, Topol EJ. The restenosis paradigm revisited: an alternative proposal for cellular mechanisms. J Am Coll Cardiol 1992;20:1284–93.
[8] Bergsma JE, de Bruijn WC, Rozema FR, Bos RR, Boering G. Late degradation tissue response to poly(L-lactide) bone plates and screws. Biomaterials 1995;16:25–31.
[9] Furie B, Furie BC. Mechanisms of thrombus formation. N Engl J Med 2008;359:938–49.
[10] Falati S, Gross P, Merrill-Skoloff G, Furie BC, Furie B. Real-time in vivo imaging of platelets, tissue factor and fibrin during arterial thrombus formation in the mouse. Nat Med 2002;8:1175–81.
[11] Kim HI, Takai M, Ishihara K. Bioabsorbable material-containing phosphorylcholine group-rich surfaces for temporary scaffolding of the vessel wall. Tissue Eng Part C Methods 2009;15:125–33.
[12] Ishihara K, Ueda T, Nakabayashi N. Preparation of phospholipid polymers and their properties as polymer hydrogel membrane. Polym J 1990;22:355–60.
[13] Ueda T, Oshida H, Kurita K, Ishihara K, Nakabayashi N. Preparation of 2-methacryloyloxyethyl phosphorylcholine copolymers with alkyl methacrylates and their blood compatibility. Polym J 1992;24:1259–69.
[14] Ishihara K. Novel polymeric materials for obtaining blood-compatible surfaces. Trends Polym Sci 1997;5:401–7.
[15] Ishihara K. Bioinspired phospholipid polymer biomaterials for making high performance artificial organs. Sci Technol Adv Mater 2000;1:131–8.
[16] Lewis AL. Phosphorylcholine-based polymers and their use in the prevention of biofouling. Colloids Surf B Biointerfaces 2000;18:261–75.
[17] Ishihara K, Goto Y, Takai M, Matsuno R, Inoue Y, Konno T. Novel polymer biomaterials and interfaces inspired from cell membrane functions. Biochim Biophys Acta, in press, doi:10.1016/j.bbagen.2010.04.008.
[18] Sawada S, Iwasaki Y, Nakabayashi N, Ishihara K. Stress response of adherent cells on a polymer blend surface composed of a segmented polyurethane and MPC copolymers. J Biomed Mater Res A 2006;79:476–84.
[19] Ishihara K, Shibata N, Tanaka S, Iwasaki Y, Nakabayashi N, Kurosaki T. Improved blood compatibility of segmented polyurethane by polymeric additives having phospholipid polar group. II. Dispersion state of the polymeric additive and protein adsorption on the surface. J Biomed Mater Res 1996;32:401–8.
[20] Hasegawa T, Iwasaki Y, Ishihara K. Preparation of blood-compatible hollow fibers from a polymer alloy composed of polysulfone and 2-methacryloyloxyethyl phosphorylcholine polymer. J Biomed Mater Res 2002;63:333–41.
[21] Long SF, Clarke S, Davies MC, Lewis AL, Hanlon GW, Lloyd AW. Controlled biological response on blends of a phosphorylcholine-based copolymer with poly(butyl methacrylate). Biomaterials 2003;24:4115–21.
[22] Ishihara K, Nomura H, Mihara T, Kurita K, Iwasaki Y, Nakabayashi N. Why do phospholipid polymers reduce protein adsorption? J Biomed Mater Res 1998;39:323–30.
[23] Kitano H, Imai M, Mori T, Gemmei-Ide M, Yokoyama Y, Ishihara K. Structure of water in the vicinity of phospholipid analogue copolymers as studied by vibrational spectroscopy. Langmuir 2003;19:10260–6.
[24] S. Chen, L. Li, C Zhao, J. Zheng. Surface hydration: principles and applications toward low-fouling/nonfouling biomaterials. Polymer 2010;51:5283–93.
[25] Ishihara K, Oshida H, Endo Y, Ueda T, Watanabe A, Nakabayashi N. Hemocompatibility of human whole blood on polymers with a phospholipid polar group and its mechanism. J Biomed Mater Res 1992;26:1543–52.
[26] Ishihara K, Ziats NP, Tierney BP, Nakabayashi N, Anderson JM. Protein adsorption from human plasma is reduced on phospholipid polymers. J Biomed Mater Res 1991;25:1397–407.
[27] Ishihara K, Aragaki R, Ueda T, Watanabe A, Nakabayashi N. Reduced thrombogenicity of polymers having phospholipid polar groups. J Biomed Mater Res 1990;24:1069–77.
[28] Snyder TA, Tsukui H, Kihara S, Akimoto T, Litwak KN, Kameneva MV, et al. Preclinical biocompatibility assessment of the EVAHEART ventricular assist device: coating comparison and platelet activation. J Biomed Mater Res A 2007;81:85–92.
[29] Yoneyama T, Sugihara K, Ishihara K, Iwasaki Y, Nakabayashi N. The vascular prosthesis without pseudointima prepared by antithrombogenic phospholipid polymer. Biomaterials 2002;23:1455–9.
[30] Yoneyama T, Ishihara K, Nakabayashi N, Ito M, Mishima Y. Short-term in vivo evaluation of small-diameter vascular prosthesis composed of segmented poly(etherurethane)/2-methacryloyloxyethyl phosphorylcholine polymer blend. J Biomed Mater Res 1998;43:15–20.
[31] Ishihara K, Iwasaki Y, Nakabayashi N. Polymeric lipid nanosphere consisting of water-soluble poly(2-methacryloyloxyethyl phosphorylcholine-co-n-butyl methacrylate). Polym J 1999;31:1231–6.
[32] Chin-Quee SL, Hsu SH, Nguyen-Ehrenreich KL, Tai JT, Abraham GM, Pacetti SD, et al. Endothelial cell recovery, acute thrombogenicity, and monocyte adhesion and activation on fluorinated copolymer and phosphorylcholine polymer stent coatings. Biomaterials 2010;31:648–57.
[33] Whelan DM, van der Giessen WJ, Krabbendam SC, van Vliet EA, Verdouw PD, Serruys PW, et al. Biocompatibility of phosphorylcholine coated stents in normal porcine coronary arteries. Heart 2000;83:338–45.
[34] Pinto Slottow TL, Waksman R. Overview of the 2007 food and drug administration circulatory system devices panel meeting on the endeavor zotarolimus-eluting coronary stent. Circulation 2008;117:1603–8.
[35] Kim HI, Takai M, Konno T, Matsuno R, Ishihara K. Biodegradable polymer films for releasing nanovehicles containing sirolimus. Drug Deliv 2009;16:183–8.
[36] Chuang TH, Stabler C, Simionescu A, Simionescu DT. Polyphenol-stabilized tubular elastin scaffolds for tissue engineered vascular grafts. Tissue Eng Part A 2009;15:2837–51.
[37] Therin M, Christel P, Li S, Garreau H, Vert M. In vivo degradation of massive poly(alpha-hydroxy acids): validation of in vitro findings. Biomaterials 1992;13:594–600.
[38] Sakai O, Nakayama Y, Nemoto Y, Okamoto Y, Watanabe T, Kanda K, et al. Development of sutureless vascular connecting system for easy implantation of small-caliber artificial grafts. J Artif Organs 2005;8:119–24.
[39] Garasic JM, Edelman ER, Squire JC, Seifert P, Williams MS, Rogers C. Stent and artery geometry determine intimal thickening independent of arterial injury. Circulation 2000;101:812–8.
[40] Sefton MV, Gemmell CH, Gorbet MB. What really is blood compatibility? J Biomater Sci Polym Ed 2000;11:1165–82.
[41] Williams DF. On the mechanisms of biocompatibility. Biomaterials 2008;29:2941–53.
[42] Boilard E, Nigrovic PA, Larabee K, Watts GF, Coblyn JS, Weinblatt ME, et al. Platelets amplify inflammation in arthritis via collagen-dependent microparticle production. Science 2010;327:580–3.
[43] Zernecke A, Bernhagen J, Weber C. Macrophage migration inhibitory factor in cardiovascular disease. Circulation 2008;117:1594–602.
[44] Jiang Y, Beller DI, Frendl G, Graves DT. Monocyte chemoattractant protein-1 regulates adhesion molecule expression and cytokine production in human monocytes. J Immunol 1992;148:2423–8.
[45] Ishii D, Schenk AD, Baba S, Fairchild RL. Role of TNF alpha in early chemokine production and leukocyte infiltration into heart allografts. Am J Transplant 2010;10:59–68.
[46] Brodbeck WG, Patel J, Voskerician G, Christenson E, Shive MS, Nakayama Y, et al. Biomaterial adherent macrophage apoptosis is increased by hydrophilic and anionic substrates in vivo. Proc Natl Acad Sci U S A 2002;99:10287–92.
[47] Sawada S, Sakaki S, Iwasaki Y, Nakabayashi N, Ishihara K. Suppression of the inflammatory response from adherent cells on phospholipid polymers. J Biomed Mater Res A 2003;64:411–6.
[48] DeFife KM, Yun JK, Azeez A, Stack S, Ishihara K, Nakabayashi N, et al. Adhesion and cytokine production by monocytes on poly(2-methacryloyloxyethyl phosphorylcholine-co-alkyl methacrylate)-coated polymers. J Biomed Mater Res 1995;29:431–9.
[49] Young TH, Lin DT, Chen LY. Human monocyte adhesion and activation on crystalline polymers with different morphology and wettability in vitro. J Biomed Mater Res 2000;50:490–8.
[50] Diaz-Guerra E, Vernal R, del Prete MJ, Silva A, Garcia-Sanz JA. CCL2 inhibits the apoptosis program induced by growth factor deprivation, rescuing functional T cells. J Immunol 2007;179:7352–7.
[51] Collier TO, Anderson JM, Brodbeck WG, Barber T, Healy KE. Inhibition of macrophage development and foreign body giant cell formation by hydrophilic interpenetrating polymer network. J Biomed Mater Res A 2004;69:644–50.
[52] Granchi D, Ciapetti G, Filippini F, Stea S, Cenni E, Pizzoferrato A, et al. In vitro cytokine production by mononuclear cells exposed to bone cement extracts. Biomaterials 2000;21:1789–95.
[53] Moro T, Takatori Y, Ishihara K, Konno T, Takigawa Y, Matsushita T, et al. Surface grafting of artificial joints with a biocompatible polymer for preventing periprosthetic osteolysis. Nat Mater 2004;3:829–36.

6．生体機能化されたチタン合金の生物学的安全性評価

国立医薬品食品衛生研究所

松岡厚子、伊佐間和郎

1．はじめに

擬似体液中でアパタイト形成能が高い医用材料は、生体内で骨と直接結合することが期待できる。近年、アパタイト形成能を付与したアルカリ加熱処理チタン合金が製品化され、さらに、より高いアパタイト形成能を付与するためにアルカリ処理したチタン合金へのカルシウム導入も図られている。そこで、我々は、骨組織適合性の高い Ti-Zr-Nb 合金にアルカリ処理後カルシウム導入のための表面処理を施し、そのアパタイト形成能を評価し、加えて、カルシウム導入した Ti-Zr-Nb 合金の細胞毒性試験及び骨芽細胞適合性試験を行って生物学的安全性を評価した。

2．実験

2.1 試験材料及び表面処理

チタン合金として、Ti と Zr の原子比を 1:1 に固定し、Nb 量が異なる Ti-Zr、Ti-Zr-4Nb、Ti-Zr-8Nb、Ti-Zr-16Nb 及び Ti-Zr-24Nb を用いた。また、対照材料として Ti-6Al-4V、純金属として Ti、Zr 及び Nb を用いた。これらの材料を NaOH 溶液を用いてアルカリ処理し、その後、$CaCl_2$ 溶液又は $Ca(OH)_2$ 溶液を用いてカルシウム導入を施した。材料表面のカルシウム導入量は、蛍光 X 線分析法（XRF）により測定した。擬似体液としてカルシウム及びマグネシウムイオンを含有するハンクス平衡塩溶液を用い、表面処理した材料を 37.0℃で 1 週間浸漬した。擬似体液浸漬後、材料表面に形成したアパタイトを、走査型電子顕微鏡（SEM）により観察し、フーリエ変換赤外光音響分光分析法（FT-IR/PAS）により定量的に解析した。

2.2 細胞毒性試験

医療機器の生物学的安全性評価のための試験法に従い、50 個のチャイニーズ･ハムスター肺由来線維芽細胞株 V79 細胞を材料ディスク（直径 14.0 mm、厚さ 1.0 mm）の上に播種し、10%牛胎児血清添加イーグル MEM 培地で 6 日間培養した。その後、ギムザ染色して形成したコロニー数を数え、コントロール群のコロニー数に対する割合（コロニー形成率）を算出した。

2.3 骨芽細胞適合性試験

正常ヒト骨芽細胞（NHOst, Cambrex CC-2538）を材料ディスクの上に播種し、5 mM β-グリセロリン酸ナトリウム及び 10% 牛胎児血清添加 α-MEM 培地で 2 週間培養した。その後、細胞増殖の指標として、WST-8 法により相対細胞数を測定した。さらに、細胞分化の指標として、パ

ラニトロフェニルリン酸を基質に用いて骨芽細胞のアルカリホスファターゼ（ALP）活性を測定した。

3．結果及び考察

3.1 カルシウム導入量

Ti-Zr、Ti-Zr-4Nb、Ti-Zr-8Nb、Ti-Zr-16Nb、Ti-Zr-24Nb、Ti-6Al-4V 及び Ti は、アルカリ処理後 $CaCl_2$ 処理に比べて、アルカリ処理後 $Ca(OH)_2$ 処理の方がカルシウム導入量が約 2 倍高かった。また、Zr は、アルカリ処理後 $CaCl_2$ 処理ではカルシウムを導入できなかったが、アルカリ処理後 $Ca(OH)_2$ 処理ではカルシウムを導入できた。また、Nb はどちらの処理法でもカルシウムを導入できなかった。

3.2 アパタイト形成能

Nb 含量にかかわらず未処理の Ti-Zr-Nb 合金は、1 週間の擬似体液浸漬によりアパタイトを形成しなかった。一方、Ti-Zr 及び Ti-Zr-4Nb は、アルカリ処理、アルカリ処理後 $CaCl_2$ 処理及びアルカリ処理後 $Ca(OH)_2$ 処理によって、アパタイトを形成した（図 1）。これらのアパタイト形成能は、アルカリ処理 < アルカリ処理後 $CaCl_2$ 処理 < アルカリ処理後 $Ca(OH)_2$ 処理の順に高くなった。さらに、Ti-Zr-8Nb は、アルカリ処理及びアルカリ処理後 $CaCl_2$ 処理ではアパタイトを形成しなかったが、アルカリ処理後 $Ca(OH)_2$ 処理によってアパタイトを形成した（図 1）。また、Ti-Zr-16Nb 及び Ti-Zr-24Nb は、いずれの表面処理でもアパタイトを形成しなかった。材料表面へのカルシウム導入量が高かった Ti-Zr-Nb 合金は、擬似体液浸漬によるアパタイト形成能も高かった。

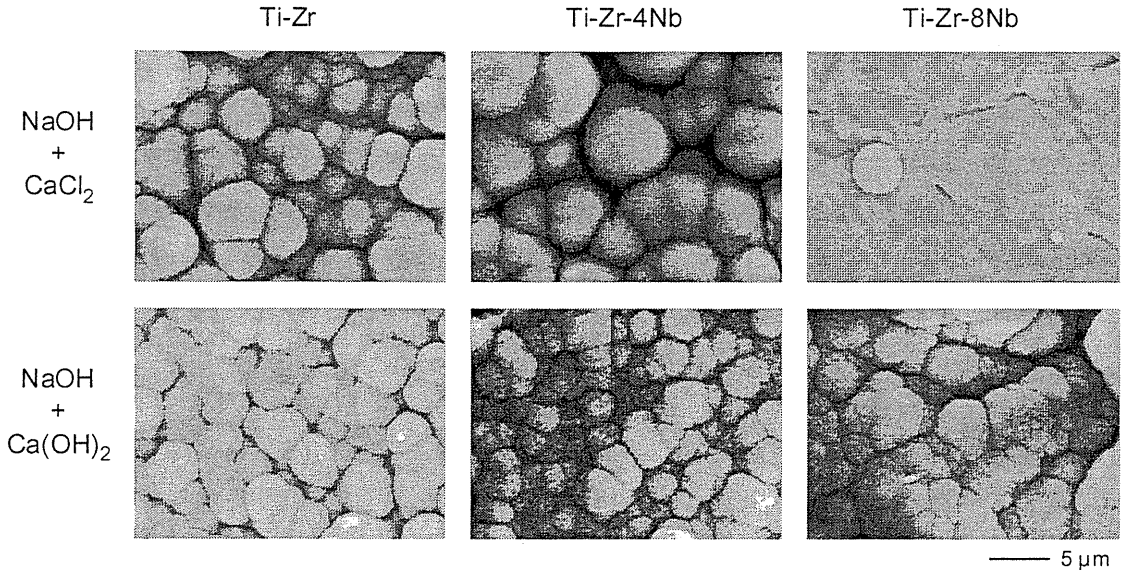

図 1　$NaOH+CaCl_2$ 処理及び $NaOH+Ca(OH)_2$ 処理した Ti-Zr、Ti-Zr-4Nb 及び Ti-Zr-8Nb のハンクス平衡塩溶液浸漬後の SEM 観察像

3.3 細胞毒性

未処理の Ti-6Al-4V は弱い細胞毒性を示したが、表面処理によって細胞毒性は問題のないレベルになった。その他の材料は、未処理及びいずれの処理においても、細胞毒性は認められなかった（図 2）。

3.4 骨芽細胞適合性

骨芽細胞の細胞数は、未処理の Ti-6Al-4V と比べて、アルカリ処理、アルカリ処理後 $CaCl_2$ 処理及びアルカリ処理後 $Ca(OH)_2$ 処理を施した Ti-6Al-4V ではいずれも増加した。その他の材料では、未処理及びいずれの処理においても骨芽細胞の細胞数に相違は認められなかった。骨芽細胞の ALP 活性は、Ti-Zr、Ti-Zr-4Nb、Ti-6Al-4V 及び Ti では、未処理、アルカリ処理、アルカリ処理後 $CaCl_2$ 処理及びアルカリ処理後 $Ca(OH)_2$ 処理の順に増加傾向が認められた。その他の材料では、未処理の Ti-6Al-4V と比べて ALP 活性は高かったものの、処理の有無による ALP 活性の相違は認められなかった。

アルカリ処理後 $Ca(OH)_2$ 処理は、Ti や Ti-Zr-Nb 合金等に高いアパタイト形成能を付与することができ、さらに、本研究で骨芽細胞の分化を促進させることが分った。Ti-Zr-Nb 合金は力学的性質にも特長があり、有効性及び安全性の高い金属材料として、埋植医療機への応用が期待できる。

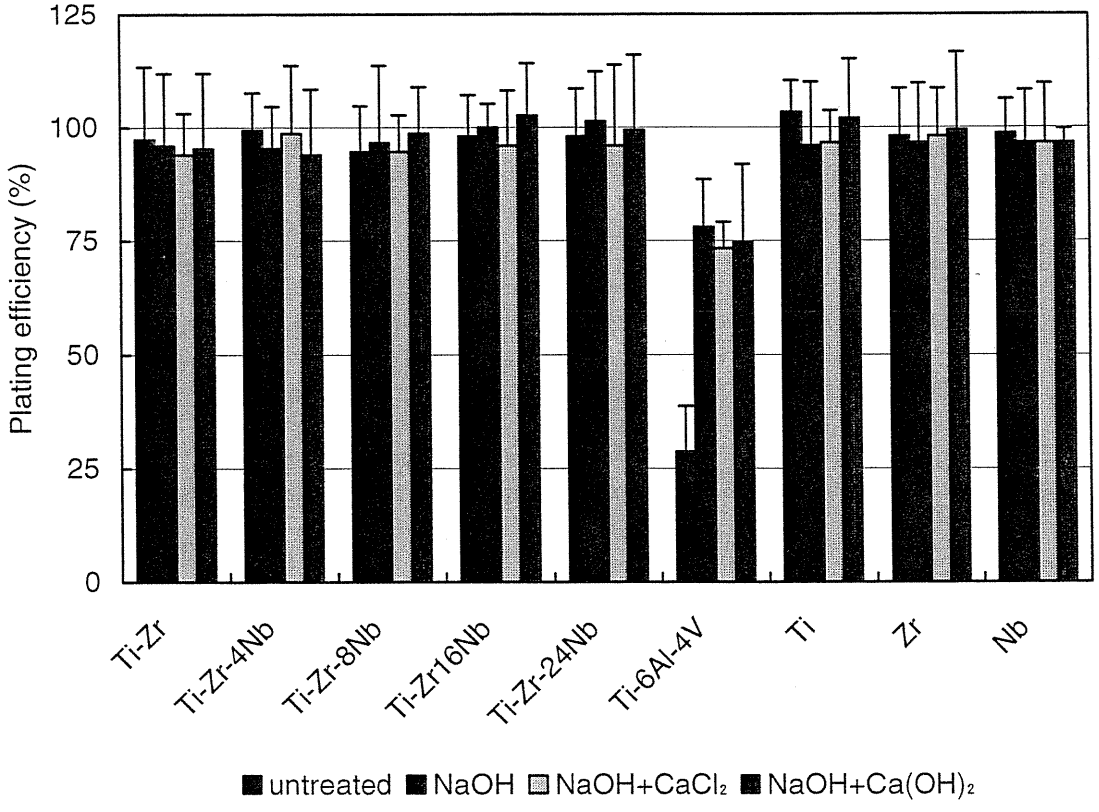

図 2　表面処理した材料のコロニー形成率

— Regular Article —

Determination of Dimethyl Fumarate and Other Fumaric and Maleic Acid Diesters in Desiccants and Consumer Products in Japan

Tsuyoshi Kawakami,*,[a] Kazuo Isama,[a] Atsuko Matsuoka,[b] and Tetsuji Nishimura[a]

[a]Division of Environmental Chemistry and [b]Division of Medical Devices, National Institute of Health Sciences, 1–18–1 Kamiyoga, Setagaya-ku, Tokyo 158–8501, Japan

(Received December 14, 2010; Accepted February 8, 2011; Published online February 18, 2011)

Recently, many contact dermatitis cases related to leather furniture and footwear containing dimethyl fumarate (DMF) as an anti-mold agent have been reported in European countries. We investigated the concentrations of DMF and several fumaric and maleic acid diesters in desiccants and household products (footwear and rack) enclosed with a desiccant sachet in Japan. We sorted the product samples by material, and analyzed the product parts that can come into contact with the skin of consumers. Twenty-one desiccant samples and eighteen product samples (seven footwear products and one rack product) were analyzed. DMF was detected in the range of 0.11–2.3 mg/kg in two desiccant samples and three product samples (different parts of one product). The DMF concentrations detected in this study exceeded the value regulated by the European Union (0.1 mg/kg); the concentration of one desiccant sample was exceeded 1.0 mg/kg which showed a strong reaction in the patch tests in a precious study. The notes printed on the sachets of the desiccant samples containing DMF read "mold-proof desiccant" and "do not eat" in one case and merely "do not eat" in the other case. DMF has strong sensitization and irritation activities; hence, it is necessary to analyze more samples to prevent DMF-related contact dermatitis in Japan. Dibutyl maleate (DBM) was detected in the rack product and enclosed desiccant; its concentration ranged from 29 to 720 mg/kg. DBM may be a constituent of the adhesive used for the rack. Further investigation is necessary to verify the cross-reaction of DBM with DMF.

Key words —— dimethyl fumarate, contact dermatitis, desiccant, footwear, mold-proof

INTRODUCTION

Dimethyl fumarate (DMF) is a white crystalline powder that undergoes sublimation at room temperature. DMF has been known as an inhibitor of mold growth and an antibacterial substance.[1,2] In addition, DMF has been used as the essential pharmaceutical component in the oral treatment of psoriasis (Fumaderm®) in Germany since 1994.[3] On the other hand, DMF is cytotoxic (epidermoid cell line A431, LD_{50}: 5.04 μg/ml), and it induces non-immunological contact urticaria and allergic contact dermatitis.[4]

Since the summer of 2006, many dermatitis cases related to leather furniture such as sofas and armchairs have been reported in European countries, especially in the U.K. and Finland.[5,6] At first, the causative substance was not identified; however the common factor in all cases was the use of leather furniture manufactured in China. In 2008, it was reported that DMF was detected in the sofas and armchairs used by the patients with contact dermatitis, and DMF was identified as the causative substance of the contact dermatitis caused by Chinese furniture.[7] After this identification of the causative substance, many cases caused by DMF have been reported; these cases are attributed not only to leather furniture but also to other consumer products such as footwear[8,9] and clothing.[10] DMF was frequently used in the desiccant sachets placed inside furniture and enclosed in footwear boxes. Evaporated DMF impregnated the products, thereby protecting them from mold. However, consumers were

*To whom correspondence should be addressed: Division of Environmental Chemistry, National Institute of Health Sciences, 1–18–1 Kamiyoga, Setagaya-ku, Tokyo 158–8501, Japan. Tel.: +81-3-3700-1141; Fax: +81-3-3707-6950; E-mail: tkawa@nihs.go.jp

adversely affected when they came into contact with the products.

DMF has been banned in products manufactured in the European Union (EU), according to the Biocide Directive (EU Directive 98/8/EC).[11] However, non-EU countries may continue using DMF as a biocide to prevent mold growth during the transport and storage of products. Since May 1, 2009, the European commission banned DMF in consumer products in the EU market (EU Directive 2009/251/EC).[12] This European directive required a DMF concentration of less than 0.1 mg/kg of the product or product part. This regulated value was considered to be sufficiently lower than the concentration (1.0 mg/kg) that showed a strong reaction in the patch test.[7] However, the number of contravention cases reported by Rapid Alert System for non-food consumer products (RAPEX),[13] which reports weekly violations of EU regulations in the EU market, exceeded 100 from May 1, 2009, to April 30, 2010. The cases related to footwear products accounted for more than 90% of all the cases.

On the other hand, to the best of our knowledge, cases of contact dermatitis related to DMF were not reported in non-EU countries, except for one case in Canada.[14] Although it is thought that similar products with sachets containing DMF are distributed in the Japanese consumer product market, contact dermatitis cases related to DMF and the amounts of DMF in desiccants and household products have not been investigated in Japan. Therefore, we investigated the concentrations of DMF in desiccants and several household products in Japan.

Furthermore, compounds having a chemical structure similar to that of DMF, such as fumaric acid diesters, maleic acid diesters, and acryl acid esters, induce contact dermatitis.[15–17] These compounds cause skin irritation and sensitization, and they also induce a cross-reaction with DMF. Therefore, in this study, we also determined the concentrations of diethyl fumarate (DEF), dibutyl fumarate (DBF), dimethyl maleate (DMM), diethyl maleate (DEM), and dibutyl maleate (DBM) in desiccants and several household products.

MATERIALS AND METHODS

Samples —— Sachets containing a desiccant were provided by volunteers who purchased footwear, bags, racks, *etc.* from retail stores in Japan. In addition, footwear products (with a desiccant sachet) were purchased from several retail stores in Japan from June to July 2010. The details of the desiccant samples and product samples are shown in Tables 1 and 2, respectively. All the desiccant samples were silica gel, except for S9 (a clay-type desiccant, Table 1). The product samples were sorted by material, and the product parts that can come into contact with the skin surface were analyzed, except for the mount paper of the rack sample (P10-3). A total of 21 desiccant samples and 18 product samples (seven footwear products and one rack product) were analyzed.

Materials —— The household products analysis grade of DMF and chemical analysis grade of DEF were obtained from Wako Pure Chemical Industries, Ltd. (Osaka, Japan). Chemical analysis grade of DBF, DMM, DEM, and DBM were obtained from Tokyo Chemical Industry Co., Ltd. (Tokyo, Japan). An environmental analysis grade of naphthalene-d_8 was obtained from Kanto Chemical Co., Inc. (Tokyo, Japan). Pesticide residue grade of ethyl acetate and methanol were obtained from Sigma-Aldrich (St. Louis, MO, U.S.A.). Silica gel powder (Silica Gel 60, particle size: 0.040–0.063 mm) used as a blank sample was obtained from Merck (Darmstadt, Germany).

Sample Processing —— The desiccant sample was crushed by an agate mortar, and 0.5 g of the sample was placed into a glass tube with 5 ml of ethyl acetate. Then, ultrasonic extraction was performed for 5 min, and the tube was centrifuged for 2 min (3000 rpm). After centrifugation, the supernatant was obtained. This extraction procedure was conducted twice. The supernatants were combined and concentrated to approximately 1 ml with a rotary evaporator while maintaining the temperature of the water bath below 40°C. Next, the solution was concentrated to below 0.5 ml by a gentle N_2 stream. Twenty-five micro liters of ethyl acetate solution containing 1 μg/ml of naphtalane-d_8 as an internal standard was added, and the sample volume was adjusted to 0.5 ml. This solution was then analyzed by GC/MS.

The product sample was cut, and 0.5 g of the sample was placed into a glass tube with 20 ml of methanol. Then, this tube was shaken for 10 min, and ultrasonic extraction was performed for 5 min. After extraction, the solution was filtered; the residue was washed with about 10 ml of methanol and the washing combined with the filtrate. The sample solution was concentrated to approximately 2 ml with a rotary evaporator while maintaining the